

## Dislocation relaxation in high-purity iron at megahertz frequencies

This article has been downloaded from IOPscience. Please scroll down to see the full text article.

1994 J. Phys.: Condens. Matter 6 8745

(<http://iopscience.iop.org/0953-8984/6/42/007>)

View [the table of contents for this issue](#), or go to the [journal homepage](#) for more

Download details:

IP Address: 171.66.16.151

The article was downloaded on 12/05/2010 at 20:49

Please note that [terms and conditions apply](#).

# Dislocation relaxation in high-purity iron at megahertz frequencies

M M Zein

University of Bahrain, Physics Department, PO Box 32038, Bahrain

Received 12 May 1994

**Abstract.** The internal-friction spectrum of high-purity polycrystalline and single-crystal iron is studied at 5, 10 and 30 MHz, over the temperature range 50–250 K. The results lead to the following conclusions: the temperature of the peak is essentially independent of the orientation; the temperature of the peak decreases with deformation and then starts to increase slightly with further deformation; the peak height increases with increasing deformation. Measurements on polycrystalline iron subjected to successive doses of neutron and  $\gamma$  irradiation showed a reduction in the relaxation strength by increasing the irradiation doses.

## 1. Introduction

In deformed high-purity BCC metals the so-called  $\alpha$  and  $\gamma$  peaks are commonly observed and believed to be associated with the intrinsic motion of dislocations [1–6]. Fantozzi *et al* [7] reviewed the role of the large difference between the mobilities of screw and edge dislocations in BCC metals on further proliferation of the peaks. Theoretical calculations have shown that the highest activation enthalpy is associated with the  $\gamma$  peak which is due to the generation of a kink pair on screw dislocations. Kink motion on screw dislocations would occur at very low temperatures and would be unlikely to be seen experimentally. More than one type of kink can occur on a dislocation, which may account for the number of peaks observed in the  $\alpha$  complex. There is no detailed study of the  $\alpha$  complex at megahertz frequencies. In the present work, a more detailed investigation of the attenuation of the longitudinal waves at frequencies of 5, 10 and 30 MHz in polycrystalline samples and single crystals with different crystallographic orientations was made in successively deformed and also successively  $\gamma$ -ray- and neutron-irradiated iron specimens.

## 2. Experimental procedures

The specimens used were 99.995 pure polycrystalline iron, and three single crystals of orientations  $\langle 111 \rangle$ ,  $\langle 110 \rangle$  and  $\langle 100 \rangle$  of the same purity (supplied by the Good-Fellow Company). The specimens were in the cylindrical form, of 10 mm length and of 13 mm diameter. The polycrystalline specimens were cut from original specimens with a low-speed diamond saw; then they were annealed for 2 h in an argon atmosphere at a temperature of 800 °C.

Successive amounts of stress were applied to the polycrystalline specimen 1 by compression using a Monsanto tensometer at room temperature. The single crystals were given a compression stress of 28 N mm<sup>-2</sup>.

Two polycrystalline specimens 2 and 3 were given a compression stress of  $62 \text{ N mm}^{-2}$  (10% deformation). Then one specimen (specimen 2) was given successive  $\gamma$ -ray doses using  $^{60}\text{Co}$  of energy 1.3 MeV at room temperature. Specimen 3 was given successive neutron doses using a neutron source (radium) which is capable of providing fast neutrons with a continuous energy spectrum extending to 10 MeV and an emission of  $10^5$  neutrons  $\text{s}^{-1}$ . All the specimens were left for 3 d at room temperature after each treatment.

Four conventional ultrasonic pulse techniques were used at frequencies of 5, 10 and 50 MHz. A short pulse of longitudinal waves, about  $1.5 \mu\text{s}$  in duration, was introduced into the specimen by means of an  $x$ -cut quartz crystal. The same transducer acted as the receiver for the reflected echoes. The echoes were amplified and displayed on an oscilloscope. The attenuation was determined by measuring the average ratio of the amplitudes of successive reflected pulses on the oscilloscope. Nonaq stopcock grease was used for an acoustic coupling between the transducer and the specimen. The temperature was measured using two platinum sensors placed close to the specimen and connected to a digital thermometer. The measurements were made with an approximately linear warm-up rate of  $0.7 \text{ K min}^{-1}$ . The damping  $Q^{-1}$  was calculated using the relation

$$Q^{-1} = 0.036\alpha C/f$$

where  $\alpha$  ( $\text{dB cm}^{-1}$ ) is the ultrasonic attenuation,  $C$  ( $\text{cm s}^{-1}$ ) is the speed of sound and  $f$  (Hz) is the frequency of measurement.

### 3. Results

#### 3.1. Single-crystal measurements

The measurements were carried out on the three single crystals with orientations close to  $\langle 110 \rangle$ ,  $\langle 111 \rangle$  and  $\langle 100 \rangle$  directions. The temperature dependence of the ultrasonic attenuation of each crystal was measured after each crystal had been given the same resolved shear stress of  $28 \text{ N mm}^{-2}$ . The results of the measurements are shown in figures 1, 2 and 3 for the three crystals at 5, 10 and 30 MHz. The measurements show that the peak occurs at almost the same temperature for the three crystals for 5, 10 and 30 MHz frequencies. Table 1 gives the summary of the results for the three crystals.

Table 1. Summary of the results for the iron crystals given a resolved shear stress of  $28 \text{ N mm}^{-2}$  at frequencies of 5, 10 and 30 MHz.

Crystallographic direction	Peak temperature $T$ (K)			Height of the peak $Q^{-1} \times 10^{-4}$		
	5 MHz	10 MHz	30 MHz	5 MHz	10 MHz	30 MHz
$\langle 111 \rangle$	77	82	93	12.28	8.089	2.35
$\langle 110 \rangle$	76	82	91	10.33	7.64	2.34
$\langle 100 \rangle$	76	83	92	10.33	7.32	1.87

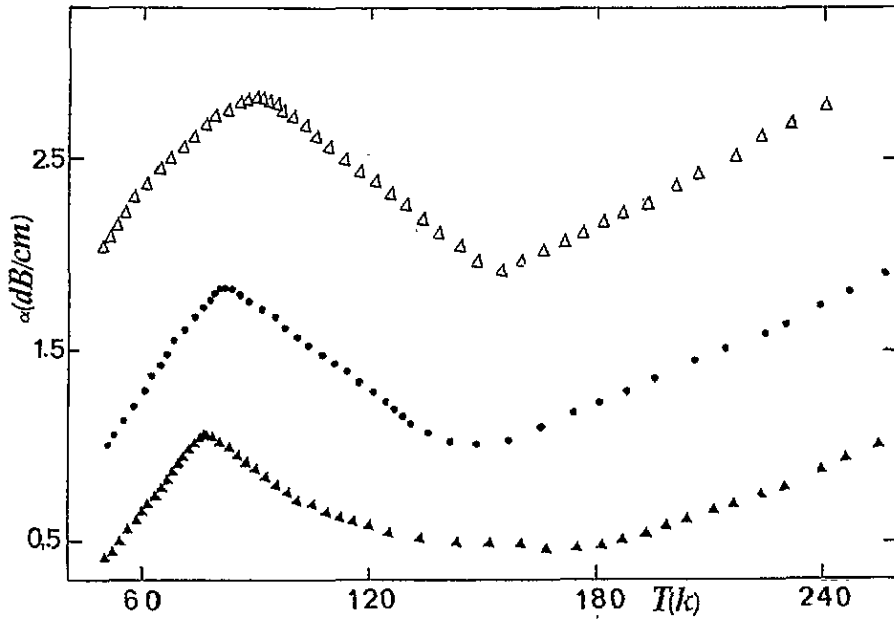


Figure 1. The ultrasonic attenuation versus temperature for a  $\{111\}$  iron single crystal of  $20 \text{ N mm}^{-2}$  resolved shear stress:  $\blacktriangle$ , 5 MHz;  $\bullet$ , 10 MHz;  $\triangle$ , 30 MHz.

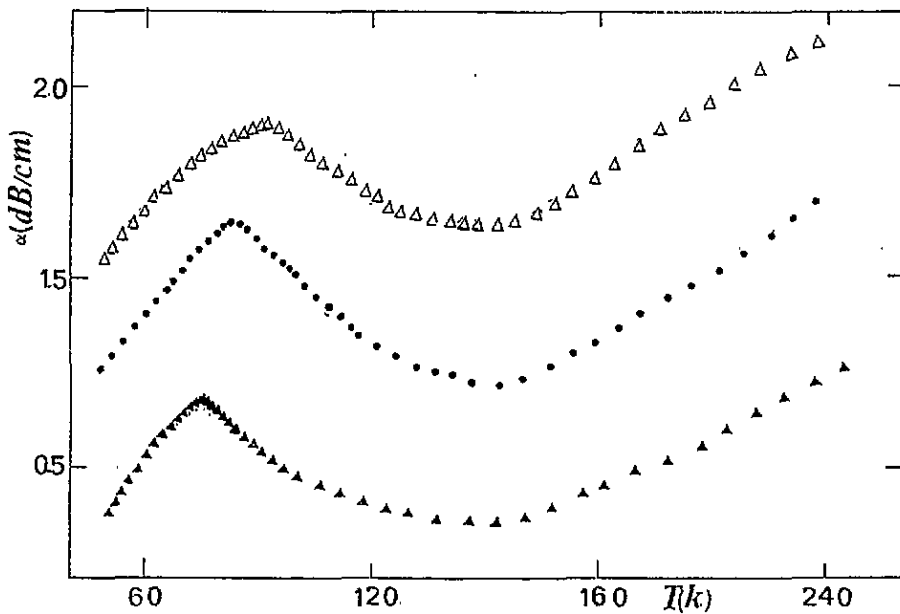


Figure 2. The ultrasonic attenuation versus temperature for a  $\{110\}$  iron single crystal of  $28 \text{ N mm}^{-2}$  resolved shear stress:  $\blacktriangle$ , 5 MHz;  $\bullet$ , 10 MHz;  $\triangle$ , 30 MHz.

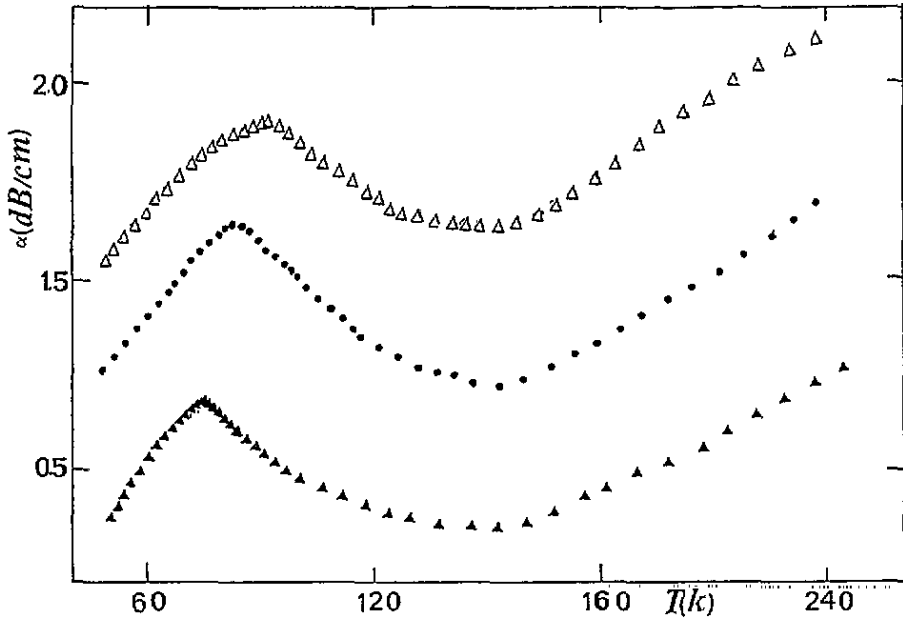


Figure 3. The ultrasonic attenuation versus temperature for a (100) iron single crystal of  $28 \text{ N mm}^{-2}$  resolved shear stress:  $\blacktriangle$ , 5 MHz;  $\bullet$ , 10 MHz;  $\triangle$ , 30 MHz.

### 3.2. Polycrystalline measurements

Figures 4 and 5 show the ultrasonic attenuation as a function of temperature for successive amounts of deformation at 10 MHz frequency; the peak occurs in the temperature range 88–82 K as deformation is increased; the figure shows an increase in the peak height as the deformation is increased.

Figures 6 and 7 show the attenuation versus temperature at 5 and 30 MHz for different amounts of stress; the results show an increase in the height of the peak with increasing stress used in the prior deformation; a shift in the peak temperature was observed as the deformation was increased. Table 2 shows the summary of the results for the polycrystalline iron specimen at the three frequencies.

### 3.3. The irradiation measurements

Figure 8 shows the results of the measurements at 10 MHz for polycrystalline iron specimen (which had been given a stress of  $60 \text{ N mm}^{-2}$ ) and then exposed to successive neutron doses from  $3.02 \times 10^9$  to  $51.28 \times 10^9 \phi nt$ . The peak occurred at a temperature between 82 and 80 K. The peak height decreased by about 60% as the neutron dose increases to  $1.8 \times 10^9 \phi nt$ . Table 3 illustrates  $Q_{\text{max}}^{-1}$  and  $T_m$  as functions of the neutron irradiation dose.

Figure 9 shows the results of the measurement at 10 MHz for the iron specimen which had been subjected to  $60 \text{ N mm}^{-2}$  and then to successive  $\gamma$  irradiations up to  $56.23 \times 10^8 \gamma vt$ ; the peak was found to occur at a temperature ranging from 82 to 79 K. The peak temperatures are slightly reduced while the peak height undergoes a reduction as the  $\gamma$  irradiation is increased. Values of  $Q_{\text{max}}^{-1}$  and  $T_{\text{max}}$  are given in table 4.

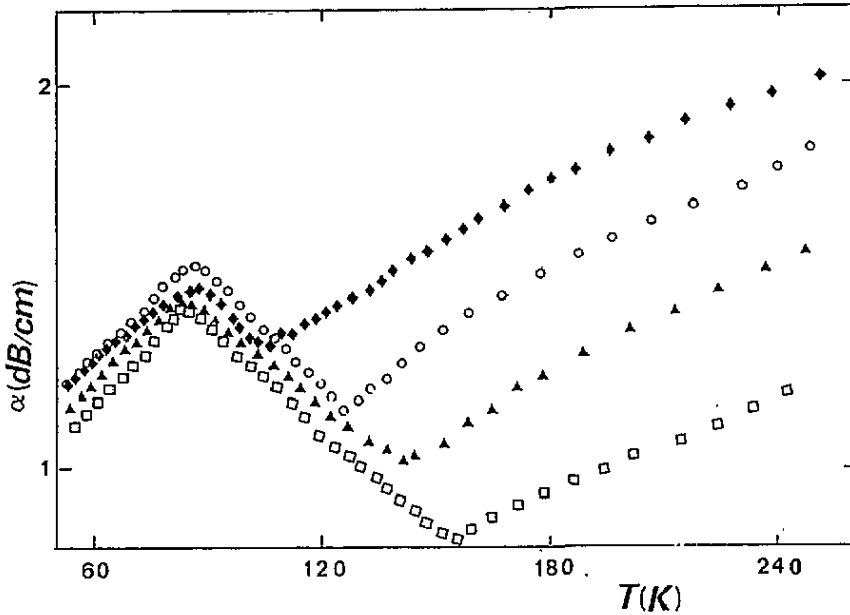


Figure 4. The ultrasonic attenuation of polycrystalline iron as a function of temperature at 10 MHz frequency:  $\blacklozenge$ ,  $0.3 \text{ N mm}^{-2}$ ;  $\circ$ ,  $3 \text{ N mm}^{-2}$ ;  $\blacktriangle$ ,  $6 \text{ N mm}^{-2}$ ;  $\square$ ,  $12 \text{ N mm}^{-2}$ .

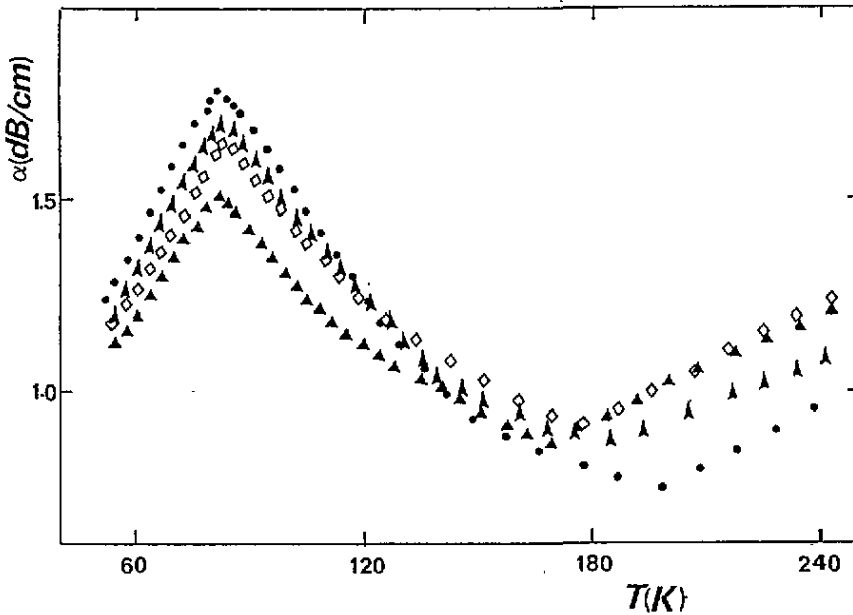


Figure 5. The ultrasonic attenuation of polycrystalline iron as a function of temperature at 10 MHz frequency:  $\blacktriangle$ ,  $31 \text{ N mm}^{-2}$ ;  $\diamond$ ,  $43 \text{ N mm}^{-2}$ ;  $\blacktriangledown$ ,  $53 \text{ N mm}^{-2}$ ;  $\bullet$ ,  $62 \text{ N mm}^{-2}$ .

Table 2. Summary of the results for polycrystalline iron at 5, 10 and 30 MHz.

$F$ (MHz)	Stress (N mm <sup>-2</sup> )	$T_{\max}$ (K)	Peak height $Q^{-1} \times 10^{-4}$
10	0.3	88	3.5
10	3	87	5.8
10	6	84	5.97
10	12.5	82	7.02
10	18	82	7.02
10	31	81	9.65
10	43	82	9.65
10	53	82	10.2
10	62	82	10.7
5	0.3	80	10.5
5	31	76	14
5	62	75	21
30	0.3	95	1.17
30	31	91	2.45
31	62	90	3.2

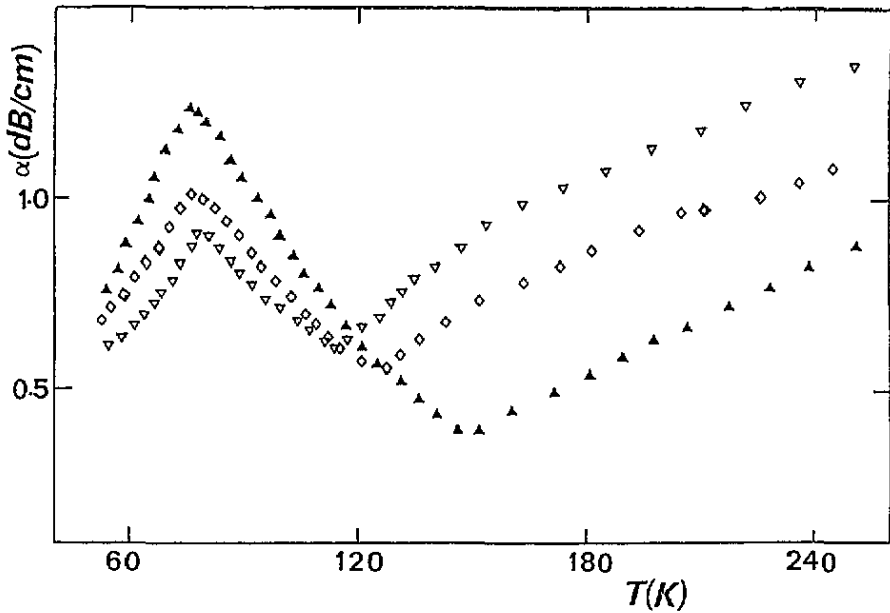


Figure 6. The ultrasonic attenuation of polycrystalline iron as a function of temperature at 5 MHz frequency:  $\nabla$ , 0.3 N mm<sup>-2</sup>;  $\diamond$ , 31 N mm<sup>-2</sup>;  $\blacktriangle$ , 62 N mm<sup>-2</sup>.

## 4. Discussion

### 4.1. The effect of crystal orientation

The measurements of 5 MHz showed that the peak occurred at 76 K, while at 10 MHz it occurred at 82 K, and at 30 MHz it was found at 92 K, for the three crystallographic

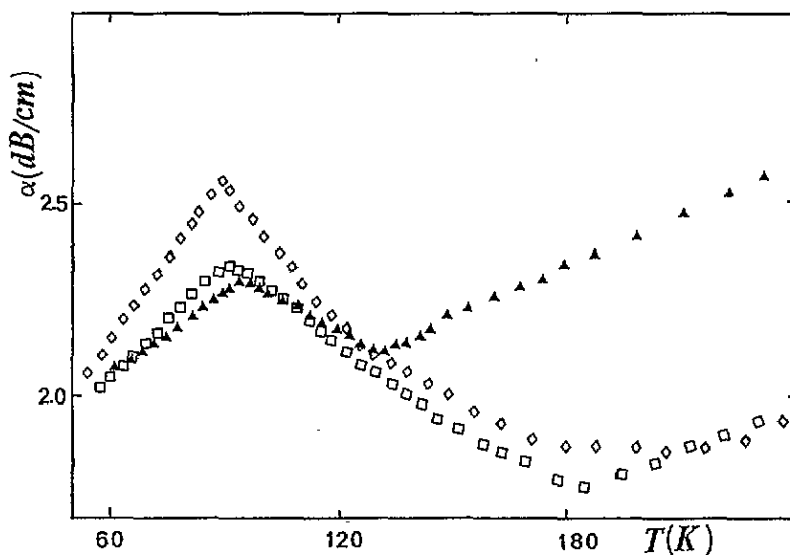


Figure 7. The ultrasonic attenuation of polycrystalline iron as a function of temperature at 30 MHz frequency:  $\blacktriangle$ ,  $0.3 \text{ N mm}^{-2}$ ;  $\square$ ,  $31 \text{ N mm}^{-2}$ ;  $\diamond$ ,  $62 \text{ N mm}^{-2}$ .

Table 3. Dependence of the  $\alpha$  peak height and its temperature on neutron dose.

Neutron dose $\times 10^9$	Peak temperature $T_{\text{max}}$ (K)	Peak height $Q^{-1} \times 10^{-4}$
—	82	10.53
3.02	82	9.82
3.715	81	8.8
5.4	80	6.7
7.2	80	5.8
9.0	80	4.8
10.8	80	4.2
12.6	80	3.7
20.89	80	2.6
36.3	80	1.9
51.28	80	1.4

direction  $\langle 111 \rangle$ ,  $\langle 110 \rangle$  and  $\langle 100 \rangle$ . The relaxation peak observed which is believed to be the  $\alpha$  peak seems to be orientation independent, similar to FCC metals. The relaxation process observed by Bordoni [8] at low temperatures in FCC metals is known to be attributed to the oscillatory motion of the edge component of dislocations on their slip planes under the influence of the periodic stress field. Obviously, the relaxation mechanism does not change when it occurs on the close-packed plane in any one direction.

#### 4.2. The effect of the frequency

We examine the effect of frequencies on the height of the peak as the frequency is increased. Table 1 gives the variation in the peak height with frequency for a specimen subjected to the same amount of stress. The peak occurred at 76 K, 82 K and 92 K when the measurements were carried at 5 MHz, 10 MHz and 30 MHz, respectively. Using these details and plotting an Arrhenius plot (figure 10), we were able to calculate the activation enthalpy and the



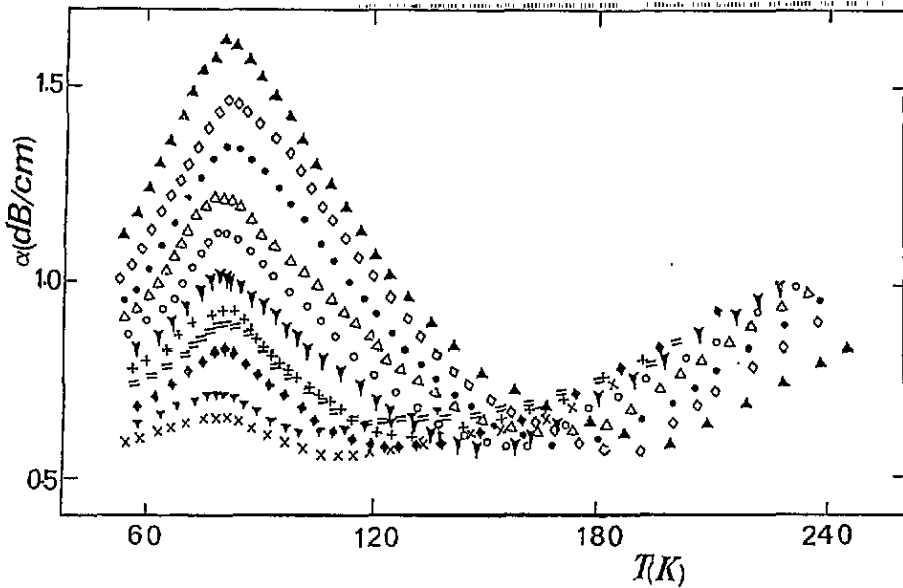


Figure 8. The ultrasonic attenuation as a function of temperature for polycrystalline iron at 10 MHz for successive doses of neutron irradiation:  $\blacktriangle$ , 0;  $\diamond$ ,  $3.02 \times 10^9$ ;  $\bullet$ ,  $3.715 \times 10^9$ ;  $\triangle$ ,  $5.4 \times 10^9$ ;  $\circ$ ,  $7.2 \times 10^9$ ;  $\nabla$ ,  $9.0 \times 10^9$ ;  $+$ ,  $10.8 \times 10^9$ ;  $=$ ,  $12.6 \times 10^9$ ;  $\blacklozenge$ ,  $36.3 \times 10^9$ ;  $\blacktriangledown$ ;  $;$ ;  $x$ ,  $51.28 \times 10^9$ .

Table 4. Dependence of the  $\alpha$  peak height and its temperature on  $\gamma$  dose.

$\gamma$ dose $\times 10^8$	Peak temperature $T_{\max}$ (K)	Peak height $Q^{-1} \times 10^{-4}$
—	82	8.78
3.23	82	7.02
4.3	82	6.30
6.45	82	5.26
8.6	81	4.56
10.75	81	3.86
14.45	80	2.8
25.75	79	2.1
56.23	79	1.2

attempt frequency for the  $\alpha$  peak which were found to be 0.069 eV and  $3.98 \times 10^9$  Hz, respectively. These values are nearly in agreement with the values reported by other workers, bearing in mind the slight variation in the amount of plastic deformation given to the sample, the thermomechanical treatment and the purity of the specimen used in their work [9].

An interesting observation is that the relaxation strength decreases as the frequency increases. It decreases by a factor of 5 as the frequency of measurement was increased from 5 to 30 MHz in nearly all the three specimens. This is in agreement with Seeger's modified theory [10, 11]; Ensouf and Fantozzi [12] applied the rate theory to kink-pair relaxation for a many-valley periodic potential. For the case of heavily deformed specimens, their calculation showed that between 1 and  $10^4$  Hz the relaxation strength  $\delta$  of the Bordoni peak decreases with increasing frequency  $f$  according to the relation

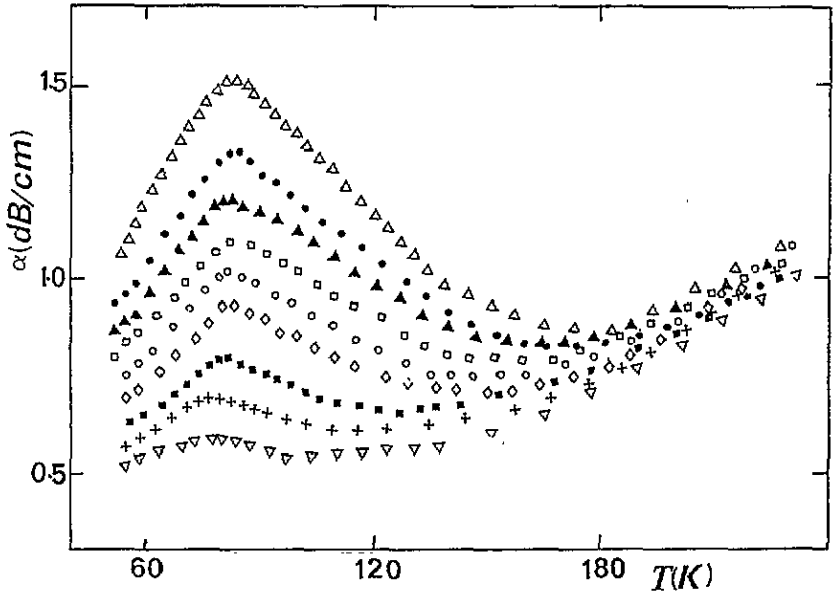


Figure 9. The variation in the ultrasonic attenuation with temperature for polycrystalline iron at 10 MHz for successive doses of  $\gamma$  irradiation:  $\Delta$ , 0;  $\bullet$ ,  $3.23 \times 10^8$ ;  $\blacktriangle$ ,  $4.3 \times 10^8$ ;  $\square$ ,  $6.45 \times 10^8$ ;  $\circ$ ,  $8.6 \times 10^8$ ;  $\diamond$ ,  $10.75 \times 10^8$ ;  $\blacksquare$ ,  $14.45 \times 10^8$ ;  $+$ ,  $25.75 \times 10^8$ ;  $\nabla$ ,  $56.23 \times 10^8$ .

$$\delta = \delta_1(1 - 0.04) \ln f$$

where  $\delta_1$  is the peak height at frequency of 2 Hz ( $\delta = Q^{-1}\pi$ ). This equation seems to be valid for high frequencies as illustrated in figure 11.

## 5. Polycrystalline measurements

### 5.1. Stress dependence

Figure 12 shows the variation in the peak height with the amount of stress used in the deformation. The peak height increases monotonically with flow stress. Most workers agree that there is a monotonic increase in the intensity of the  $\alpha$  relaxation as a function of plastic deformation in BCC metals. Tokita and Salcanoto [13], Garcia *et al* [14], Zein and Alnaser [1], Gibala *et al* [15], Korenko *et al* [16] and Amatean *et al* [17] have shown that the intensity of the  $\alpha$  relaxation is proportional to the flow stress. This is, in turn, proportional to the dislocation density [18, 19]. It can be concluded that the intensity of the  $\alpha$  relaxation is associated with the dislocation density which is expected to increase at higher deformations. This is also supported by the kink-pair generation theory proposed by Seeger [20–23] which predicted an increase in the peak (Bordoni) with increasing plastic deformation.

Figure 13 shows the variation in the peak temperature with deformation. The peak occurs at 88 K for lightly deformed specimens. This temperature decrease to about 81 K as the stress increased to  $31 \text{ N mm}^{-2}$ ; further deformation caused the temperature of the peak to increase to about 82 K. This decrease in the peak temperature was reported for BCC metals by Zein and Alnaser [1], Korenko *et al* [16] and Stanley and Szkoiak [24]

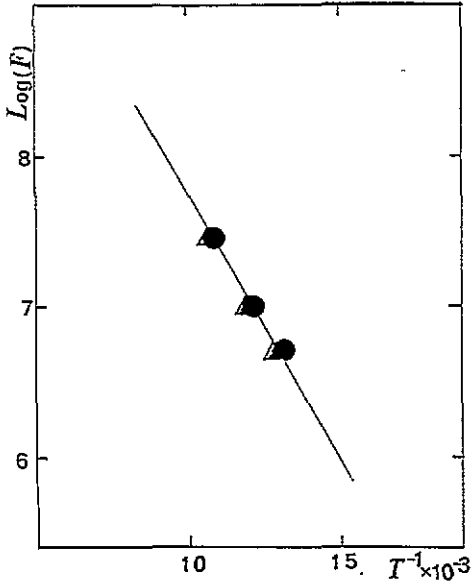


Figure 10. Frequency dependence of the temperature of the peak for single-crystal iron.

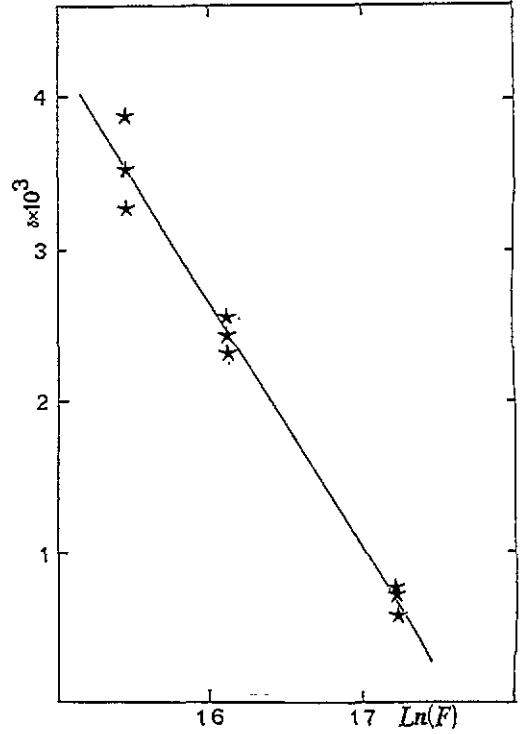


Figure 11. The variation in the height of the peak as a function of stress used in the prior deformation.

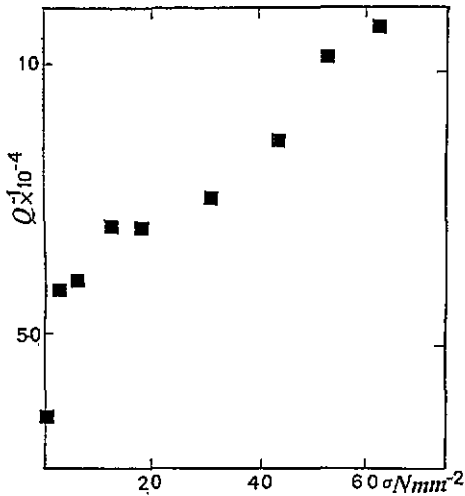


Figure 12. The variation in the temperature of the peak with the stress used in the prior deformation.

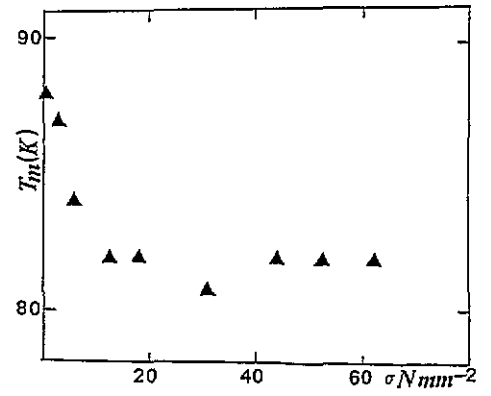


Figure 13. The relation between the peak height and neutron irradiation doses.

as the amount of plastic deformation is increased. The variation in the peak temperature

with stress is in quantitative agreement with Seeger's theory as modified by Paré [25] and Engelke [11] to take into account the different internal stresses and dislocation loop lengths present at different deformations.

In view of the variation in the peak temperature with deformation it is important to compare results at different frequencies on a similarly stressed specimen when attempting to determine the activation energy of the relaxation process. We found that the activation energy decreases with increasing deformation. Table 5 gives the variation in the activation energy with the stresses given in the prior deformation.

Table 5. The variation in activation energy with the stresses used in the prior deformation.

Stress (N mm <sup>-2</sup> )	$W_k$ (eV)	$F_0$ (Hz)
0.3	0.077	$7.9 \times 10^9$
31	0.073	$4.8 \times 10^9$
62	0.069	$4.26 \times 10^9$

### 5.2. Effect of irradiation

The peak height decreases very dramatically on irradiation. Also the irradiation reduced the peak temperature. From the study of the  $\alpha$  peak in BCC metals, Gran [26], Garcia *et al* [14], Seeger and Wuthrich [27] and Wuthrich [28] suggest that the geometrical kink migration on screw dislocations would remain possible explanations for the mechanical loss damping which occurs at low temperatures. This means that the strength of the relaxation peaks is highly dependent on the dislocation loop length introduced in the crystal. Introducing pinning points in the dislocation loop will shorten the loop and therefore the relaxation strength will be less. This is clearly observed in our work. In comparison with the Bordoni peak in FCC metals our results can be interpreted by using Paré's [25] model which showed that the peak temperature  $T_m$ , the free-dislocation loop length  $L$ , the activation energy  $W$  and the internal stress  $\sigma_1$  are interrelated. He reported this observation using the condition

$$\sigma_1 Lab \geq W \quad (1)$$

where  $W$  is the activation energy for the formation of a pair of kinks  $a$  is the atomic distance and  $b$  is the Burgers vector. The term  $\sigma_1 Lab$  is the work done in moving the dislocation loop from the straight to the deformed position.  $W$  is related to  $T_m$  by

$$f = f_0 \exp\left(-\frac{W}{kT_m}\right) \quad (2)$$

where  $f$  is the frequency of measurement,  $f_0$  is the attack frequency and  $k$  is the Boltzmann constant. Irradiation shortens the length of the dislocation segments. Paré's condition is then fulfilled only by those segments that are exposed to large internal stresses. According to Donth [29], those segments have a lower activation enthalpy so that the damping maximum is shifted to a lower temperature. Engelke [11] supported Paré's theory and concluded that the peak temperature decreases as a result of shortening the dislocation loop length or increasing the internal stresses. Most Bordoni peak theories suggest that the peak height is dependent on the dislocation density and the dislocation loop length of the form

$$Q_{\max}^{-1} \propto \Delta L^n \quad (3)$$

where  $n$  varies between 1 and 2 [9, 25, 30]. The dependence of the dislocation loop length on the concentration  $C$  of point defects was assumed to be inversely proportional, i.e.

$$L \propto C^{-\gamma} \tag{4}$$

Combining equations (3) and (4), and assuming that  $L$  is constant give

$$\log Q_{\max}^{-1} \simeq \text{constant} - n\gamma \log C \tag{5}$$

On the assumption that  $C$  is proportional to irradiation dose  $D$  (neutron dose  $D_n$  or  $\gamma$  dose  $D_\gamma$ ), equation (5) could be written as

$$\log Q_{\max}^{-1} \simeq \text{constant} - n\gamma \log D_{n,\gamma}$$

where  $n$  and  $\gamma$  are integers. This relation is plotted in figures 13 and 14.

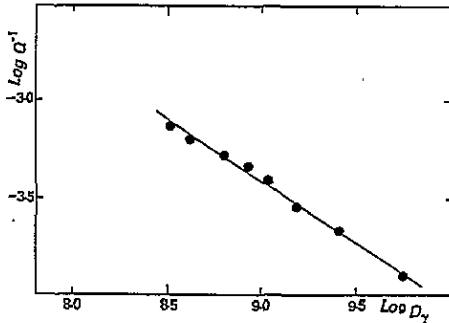


Figure 14. The relation between the peak height and the  $\gamma$  irradiation doses

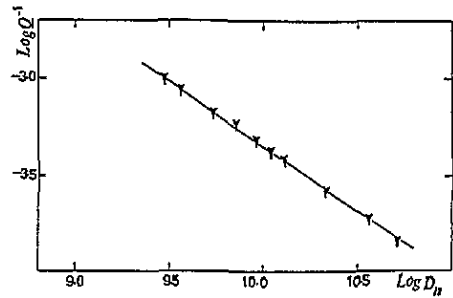


Figure 15. The relation between the peak height and the  $n$  irradiation doses.

We found that  $n\gamma = -0.58$  for neutron irradiation and  $n\gamma = -0.65$  for  $\gamma$  irradiation. Hence

$$Q_{\max}^{-1} \propto \Lambda D_n^{-0.58}$$

$$Q_{\max}^{-1} \propto \Lambda F_\gamma^{-0.65}$$

This means that the relaxation strength is more affected by  $\gamma$  than by neutron irradiation. This is probably due to the high-energy electrons, which result from the Compton effect process within the specimen that was irradiated by  $\gamma$  particles and which are more likely to reach the dislocation loops and pin them.

This clearly explains the linear drops in peak height as the irradiation doses were increased.

### 6. Conclusions

The results lead to the following.

- (1) The  $\alpha$  peak in iron has the same character as the Bordoni peak in FCC metals.
- (2) The temperature of the peak is essentially independent of the orientation.
- (3) The peak height increases with increasing deformation.
- (4) The temperature of the peak decreases with deformation and then increases slightly on further deformation.
- (5) The activation enthalpy decreases with increasing deformation.

## References

- [1] Zein M M and Alnaser W E 1993 *J. Phys.: Condens. Matter* **5** 5225-34
- [2] Alnaser W E and Zein M M 1992 *Solid State Commun.* **83** 495-500
- [3] Alnaser W E and Zein M M 1991 *Phil. Mag. A* **64** 613-8
- [4] Zein M M and Alnaser W E 1993 *Mater. Sci. Forum* **119-21** 207-12
- [5] Chambers R H 1968 *Physical Acoustics* vol 3A, ed W P Mason (New York: Academic) p 123
- [6] Fantozzi G and Ritchie I G 1981 *J. Physique* **42** C5 3
- [7] Fantozzi G, Beniot W, Esnouf C and Perez J 1979 *Ann. Phys., Paris* **47**
- [8] Bordoni P G 1949 *Ricerca Scient.* **19** 351
- [9] Fantozzi G, Esnouf C, Benoit W and Ritchie I G 1982 *Prog. Mater. Sci.* **27** 311-451
- [10] Engelke H 1969 *Phys. Status Solidi* **36** 231
- [11] Engelke H 1969 *Phys. Status Solidi* **36** 245
- [12] Esnouf C and Fantozzi G 1978 *Phys. Status Solidi a* **47** 201
- [13] Tokita K and Sakanoto K 1979 *Scr. Metall.* **4** 403-8
- [14] Garcia J A, Lomer J N and Sutton C R 1986 *Phil. Mag. A* **53** 773
- [15] Gibala R, Korenko M K, Amateau M G and Mitchell T E 1970 *J. Phys. Chem. Solids* **31** 1889
- [16] Korenko M K, Mitchell T E and Gibala R 1974 *Acta Metall.* **22** 649
- [17] Amateau M F, Mitchell T E and Gibala R 1969 *Phys. Status Solidi* **36** 407
- [18] Lowley M F and Gaigher H L 1964 *Phil. Mag.* **10** 15
- [19] Taylor G and Christain J W 1967 *Phil. Mag.* **15** 893
- [20] Seeger A 1955 *Phil. Mag.* **46** 1194
- [21] Seeger A 1956 *Phil. Mag.* **1** 651
- [22] Seeger A 1971 *J. Physique* **32** C2 193
- [23] Seeger A 1981 *J. Physique* **42** C5 214
- [24] Stanley M W and Szkoiaik Z C 1967 *J. Mater. Sci.* **2** 559
- [25] Paré V K 1961 *J. Appl. Phys.* **28** 332
- [26] Gran R 1981 *Thesis* Stuttgart University
- [27] Seeger A and Wuthrich C 1976 *Nuovo Cimento B* **33** 38
- [28] Wuthrich C 1975 *Scr. Metall.* **9** 641
- [29] Donth H 1957 *Z. Phys.* **149** 111
- [30] Grandchamp P A 1971 *Physica* **32** 2